Environmental Science and Pollution Research (2020) 27:9935–9942
https://doi.org/10.1007/s11356-019-07547-z

RESEARCH ARTICLE

Synthesis of CuCe co-modified mesoporous ZSM-5 zeolite for the selective catalytic reduction of NO by NH_3

Yuanyuan Ma[1,2] · Yang Liu[1] · Zhifang Li[3] · Cui Geng[3] · Xuefeng Bai[1] · Dianxue Cao[4]

Received: 7 August 2019 / Accepted: 29 December 2019 / Published online: 11 January 2020

Abstract

Mesoporous ZSM-5 zeolite (MZ) was used as support for Cu and Ce species, and the effects of structure and physical-chemical properties on selective catalytic reduction of NO with NH_3 (NH_3-SCR) were investigated. The characterization and experimental results show that the high activity of the Cu-Ce/MZ catalyst could be due to its high surface area, more and uniformly distributed active sites, and abundant oxidative species. Compared with the conventional ZSM-5 and SBA-15, the Cu-Ce/MZ possesses large amount of mesopores, and more accessible active sites, which are beneficial to accelerate the diffusion and improve the internal mass transfer in the denitration process. The Cu-Ce/MZ catalyst shows higher activity than Cu-Ce/ZSM-5 and Cu-Ce/SBA-15 at 200 °C.

Keywords Mesoporous ZSM-5 · Selective catalytic reduction · Surface area · CuCe co-modified

Introduction

The selective catalytic reduction of ammonia (NH_3-SCR) is the most efficient technology for removing NO_x from diesel engines (Busca et al. 1998). Although conventional three-way catalyst of V_2O_5/WO_x–TiO_x (Song et al. 2016) has been used for decades to control NO_x emissions from diesel engine exhaust, it has some inevitable drawbacks that restricted their application, such as the narrow temperature operation window (300–400 °C), low thermal stability resulting from the phase transformation of TiO_2, and the toxicity of vanadium species (Heck 1999; Shi et al. 2011). Metal-exchanged microporous zeolites have received much attention recently due to their high catalytic activity, wide temperature window, and outstanding structural durability (Beale et al. 2015; Dusselier and Davis 2018; Zhang et al. 2016).

Since Cu/ZSM-5 has been regarded as one of the most effective zeolite catalysts for the decomposition of nitrogen oxides (Iwamoto et al. 1986), researchers have carried out a lot of work to improve the performance in the NH_3-SCR, such as active reaction temperature, copper species, active sites, intermediates, and catalyst promoters in the NH_3-SCR reaction. Due to CeO_2 having high oxygen storage capacity, excellent redox properties, and strong interactions with other metals, it is introduced to Cu/ZSM-5 to enhance the catalytic activity and hydrothermal stability (Pang et al. 2014; Wang et al. 2017). Moreover, the micropore structure of zeolite leads to the diffusion limitations, poor dispersion, and inaccessibility of the catalytically active centers (Chal et al. 2011; Holm et al. 2011; Ma et al. 2013; Serrano et al. 2013). The generation of mesopores can modify the structure of the zeolite and enhance catalytic efficiency. Compared with conventional microporous zeolites, the mesoporous zeolites exhibit higher activity at low temperatures and stability in the long term (Góra-Marek et al. 2015; Rutkowska et al. 2015; Yue et al. 2015c).

The synthesis routes used to prepare mesoporous zeolites include template methods (Liu et al. 2016; Xie et al. 2016; Yan

Responsible editor: Santiago V. Luis

Electronic supplementary material The online version of this article (https://doi.org/10.1007/s11356-019-07547-z) contains supplementary material, which is available to authorized users.

✉ Xuefeng Bai
xuefengbaishy@163.com

✉ Dianxue Cao
caodianxue@hrbeu.edu.cn

[1] Institute of Petrochemistry, Heilongjiang Academy of Sciences, Harbin 150040, Heilongjiang Province, China

[2] College of Chemistry and Chemical Engineering, Qiqihar University, Qiqihar 161006, Heilongjiang Province, China

[3] College of Materials Science and Engineering, Qiqihar University, Qiqihar 161006, Heilongjiang Province, China

[4] College of Material Science and Chemical Engineering, Harbin Engineering University, Nantong St #145, Harbin 150001, China

et al. 2016; Yue et al. 2015a) and post-treatments (Ma et al. 2013; Rutkowska et al. 2017; Vennestrøm et al. 2011) for NH_3-SCR technology. However, the template methods suffer from template removal problem and impurity introduction. The post-treatments usually change the acidity and crystalline framework of zeolites and result in material loss.

To reduce the diffusional distance and enhance the loading of metal ions, another direct way is to decrease the crystal size of zeolites so as to increase the surface area. Wakihara et al. (Peng et al. 2018) reported that nanosized SSZ-13 zeolite with strong hydrothermal stability was prepared by a two-stage synthetic method, which displayed the same catalytic performance in the NH_3-SCR reaction as the micro-scale counterparts. Tsunoji et al. (Takata et al. 2016) synthesized nanosized CHA zeolites with high thermal and hydrothermal stability by the hydrothermal transformation of FAU zeolites in the presence of N, N, N-trimethyl-1-adamantammonium hydroxide (TMAdaOH), and the obtained Cu-loaded nanosized CHA zeolite catalyst showed good performance for the NH_3-SCR even after hydrothermal treatment at 900 °C for 4 h.

The ZSM-5 zeolite modified with Cu and Ce has attracted a lot of concern in recent years due to its good performance in the NH_3-SCR reaction. Therefore, it is beneficial to prepare Cu, Ce co-modified mesoporous ZSM-5 zeolite with nanosized particles. In this work, mesoporous ZSM-5 zeolite assembled with nanocrystals was prepared by one-pot hydrothermal crystallization method in the presence of urea. The obtained mesoporous ZSM-5 was incorporated with Cu and Ce by ion-exchange method. The Cu, Ce co-modified mesoporous ZSM-5 zeolite showed excellent catalytic activity compared with conventional ZSM-5 and SBA-15 molecular sieves in the NH_3-SCR reaction.

Experimental

Catalyst preparation

In a typical synthesis, 0.28 g aluminum sulfate octadecahydrate ($Al_2(SO_4)_3$•$18H_2O$) and 6.25 mL tetrapropylammonium hydroxide solution (TPAOH, 25%) were mixed with 3.75 mL of distilled water and stirred until clear. Five-milliliter tetraethyl orthosilicate (TEOS) was then added under vigorous stirring for 6 h at room temperature. Next, 0.01 g sodium fluoride was added into the mixture and stirred for 0.5 h. The homogenous solution has the following molar ratios: 1 Al_2O_3: 50 SiO_2: 8 TPAOH: 0.42 NaF: 1500 H_2O. The obtained ZSM-5 precursor was mixed with the required amount of urea aqueous solution (0.165 g urea dissolved in 15 mL water). After stirring for another 30 min, the resultant gel mixture was transferred into Teflon-lined autoclave and heated at 100 °C for 48 h. To completely remove the templates, the collected precipitate was filtered, dried in air, and calcined at 550 °C for 6 h to obtain Na/MZ. This material was further ion-exchanged with a 0.1 M NH_4NO_3 solution at 80 °C for three times, followed by calcination at 500 °C for 5 h to form H/MZ. Subsequently, 1.0 g H/MZ material was ion-exchanged with 0.0075 M $Cu(NO_3)_2$ and 0.0075 M $Ce(NO_3)_3$ solution in 150 mL water at 80 °C for 2 h under stirring. To ensure complete exchange, this procedure was repeated three times. The resulting materials calcined in static air at 550 °C for 6 h were denoted as Cu-Ce/MZ in the following.

For comparison, we also prepared conventional ZSM-5. The synthesis steps were similar to those described above, with the exception that urea was not used. SBA-15 (Si: Al = 25) was also synthesized according to the literature (Wu et al. 2006). The ion-exchange method was applied to generate Cu-Ce/ZSM-5 and Cu-Ce/SBA-15 as above.

Catalyst characterization

X-ray diffraction (XRD) analysis of the samples was carried out employing Cu Kα ($\lambda = 0.15418$ nm) radiation on the Shimadzu XRD-6000 diffractometer (Shimadzu, Japan) under the setting conditions of 40 kV, 30 mA, and a scan range from 5 to 40° with a scanning velocity of 5° min^{-1}.

N_2 adsorption/desorption isotherms were performed on a Quantachrome Autosorb iQ (Quantachrome, USA). Prior to the analysis, the samples were degassed at 573 K for 3 h. The elemental analysis was performed on inductively coupled plasma mass spectrometry (ICP-MS, Agilent 7500ce).

Transmission electron microscopy (TEM) was conducted by a HITACHI H-8100 electron microscope (Hitachi, Japan) operated at an accelerating voltage of 200 kV.

The X-ray photoelectron spectroscopy (XPS) measurements were performed on a Thermo ESCALAB 250Xi spectrometer (Thermo, USA), equipped with a monochromatized Al Ka X-ray source (1486.6 eV) and passing energy of 20 eV. The C 1-s peak (binding energy 284.8 eV) of adventitious carbon was used as a reference. XPS data from regions related to the Cu 2p and/or Ce 3d core levels were acquired.

Ammonia temperature–programmed desorption (NH_3-TPD) was analyzed by the TP 5000-II multiple adsorption apparatus (Xianquan, China). The samples (~ 0.1 g) were pretreated at 500 °C for 60 min in the He flow, then cooled down to 100 °C and adsorbed ammonia for 30 min. Ammonia desorption was measured at a rate of 10 °C/min in the temperature range of 100–500 °C.

Catalytic test

The NH_3-SCR activity of the samples was determined in a fixed bed quartz reactor at atmospheric pressure. A total of 300 mg catalyst was used in each run. The reactant gas consisted of 500 ppm NO, 500 ppm NH_3, 5% O_2, and balanced with N_2. The total flow rate was 100 mL/min.

All data were recorded at the desired temperature for 50 min to achieve a stable state. The NO and NO_2 concentrations were continually monitored by a flue gas analyzer (MRU OPTIMA7). The NO conversion was measured based on the following equations:

$$\text{NO conversion } [\%] = \frac{[\text{NO}]\text{inlet} - [\text{NO}]\text{outlet}}{[\text{NO}]\text{inlet}} \times 100\ [\%]$$

Results and discussion

XRD patterns

The XRD patterns of the Na/MZ, Cu-Ce/MZ, and Cu-Ce/ZSM-5 samples are shown in Fig. 1. All samples exhibit a typical MFI diffraction peak, which indicates that the original zeolite structure remains intact. However, the intensity of the diffraction peaks has significant differences. For Cu-Ce/MZ, the intensity of peaks decreases compared with those of Na/MZ, but the shift of peak position and diffraction peaks caused by Cu or Ce related compound or metal copper cannot be observed. These results indicate that the zeolite structures cannot be significantly influenced by the ion exchange processes and subsequent calcination treatment, and crystalline CuO_x, CeO_x, or Cu are not formed or rarely formed. The ion-exchange method can effectively disperse cupric and cerium ions in the zeolite framework (Song et al. 2015). The peak intensity for Cu-Ce/MZ after the ion-exchange process decreases, which demonstrates that the crystallinity decreases (Shan et al. 2008). The diffraction pattern of Cu-Ce/ZSM-5 zeolite is compared and analyzed, indicating the high crystallinity of microporous zeolite. The addition of Cu and Ce does not affect the mesoporous structure of Cu-Ce/SBA-15 as shown in Fig. S1.

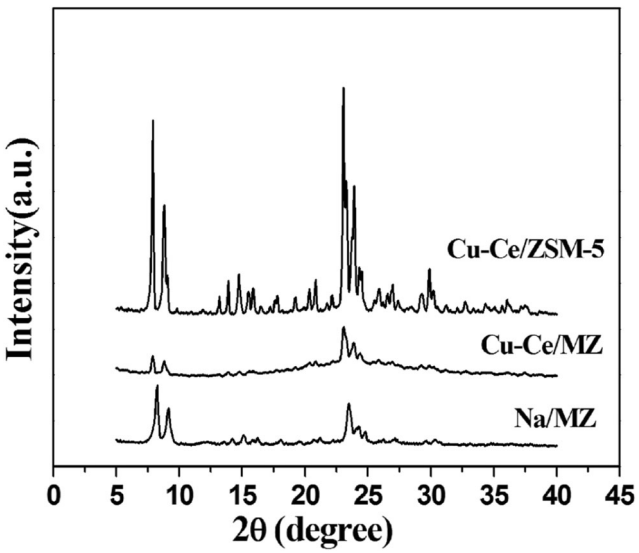

Fig. 1 XRD patterns of the Na/MZ, Cu-Ce/MZ, and Cu-Ce/ZSM-5 samples

N_2 adsorption-desorption results

N_2 adsorption-desorption isotherms of the Na/MZ, Cu-Ce/MZ, Cu-Ce/ZSM-5, and Cu-Ce/SBA-15 are depicted in Fig. 2, and their textural properties are illustrated in Table 1. The conventional Cu-Ce/ZSM-5 shows a type-I isotherm of microporous materials, and the BET surface area and total pore volume are calculated to be 340.3 m^2/g and 0.26 cm^3/g, which shrink slightly relative to the ZSM-5 (396.6 m^2/g, 0.27 cm^3/g). In contrast, Cu-Ce/MZ catalyst exhibits type-IV isotherm and H1 hysteresis loops in the region $0.45 < P/P_0 < 0.85$ due to the capillary condensation in the mesopores. It is clear that the addition of urea generates significant changes to the mesopore structures. The hysteresis loop of the Na/MZ without ion-exchange slightly shifts to a lower relative pressure ($0.40 < P/P_0 < 0.80$), which indicates a smaller pore diameter, as shown in Table 1. The surface area (S_{BET}), meso surface area (S_{meso}), total volume (V_{total}), and micro volume (V_{micro}) of the parent zeolitic supports are 669.4 m^2/g, 591.5 m^2/g, 0.70 cm^3/g, and 0.03 cm^3/g for Na/MZ, and 512.8 m^2/g, 459.0 m^2/g, 0.68 cm^3/g, and 0.02 cm^3/g for Cu-Ce/MZ after the ion-exchange treatment, respectively. It is estimated that with the ion-exchange treatment, the pore structure of Cu-Ce/MZ samples was influenced slightly. The reduction of BET surface area and microporous volume is due to small oxide aggregates on the external surface, which partially block the zeolite pores and channels. These results indicate that metal ions are incorporated into the micropore space of H/MZ (Li et al. 2013). This further demonstrates that Cu-Ce/MZ possesses microporous/mesoporous structure and large specific surface area, which should increase the active components and benefit the diffusion-controlled reactions. In addition, Cu-Ce/SBA-15 exhibits a type-IV isotherm of mesoporous materials, and the BET surface area and total pore volume significantly decrease (404.4 m^2/g, 0.76 cm^3/g) after ion-exchange treatment compared with SBA-15 (684.7 m^2/g, 0.78 cm^3/g). This illustrates that SBA-15 with mesoporous has poor stability. N_2 adsorption-desorption isotherms of ZSM-5 and SBA-15 are shown in Fig. S2.

TEM imaging

The micro-morphology of the catalysts is characterized by TEM. The TEM image (Fig. 3a) of Cu-Ce/MZ shows the existence of disordered worm-like mesoporous structure, which should be beneficial for diffusion. Additionally, dark spots with sizes in the range of 10–20 nm are clearly visible due to the presence of metal oxide nanoparticles, which are highly dispersed without obvious agglomeration after ion-exchanged treatment. Similar conservation of metal oxide nanoparticles can be observed in Cu-Ce/SBA-15, while

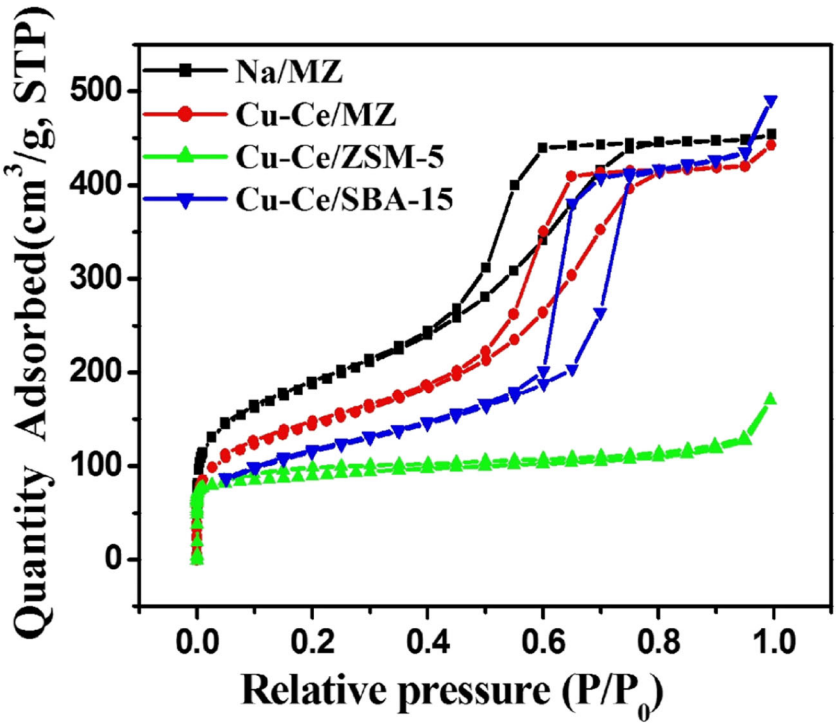

Fig. 2 N_2 adsorption-desorption isotherms of the samples: Na/MZ, Cu-Ce/MZ, Cu-Ce/ZSM-5, and Cu-Ce/SBA-15

the 2D hexagonal mesoporous structure can also be preserved after metal loading (Fig. 3b). As TEM did not further illustrate the state and content of the metal oxide nanoparticles, a more detailed evaluation of the intrapore metal oxide species was accomplished by ICP-MS investigations (Table 1) and XPS analysis.

XPS analysis

XPS analysis was undertaken to elucidate atomic concentrations on the surface and chemical state of Cu and Ce in the Cu-Ce/MZ, Cu-Ce/SBA-15, and Cu-Ce/ZSM-5 samples. The XPS spectra of Cu $2p_{3/2}$ and Ce 3d of various catalysts are shown in Fig. 4, and the results are shown in Table 2. Figure 4 a displays the Cu $2p_{3/2}$ spectra, with peaks centered at 933.6 and 932.5 eV corresponding to Cu^{2+} and Cu^{+}, respectively (Boningari et al. 2015). The results indicate that CuO and Cu_2O species may be present in the Cu-Ce/MZ, Cu-Ce/SBA-15, and Cu-Ce/ZSM-5 samples. The XPS spectra of the Ce 3d peaks are shown in Fig. 4b. The peaks located at 905.0 eV are arised from $Ce^{3+}3d_{3/2}$, and the peaks located at 884.4 eV are arised from $Ce^{3+}3d_{5/2}$, while the others can be assigned unambiguously to Ce^{4+} species (Song et al. 2015). The atomic concentrations of Cu and Ce on the surface of Cu-Ce/MZ are 0.05% and 0.11%, respectively, as presented in Table 2. Ce has high redox ability ($Ce^{3+} \leftrightarrow Ce^{4+}$), excellent oxygen storage capacity, abundant oxygen vacancies, and oxygen ion transport characteristics, so the addition of Ce can increase the oxygen adsorption and promote the conversion of NO to NO_2 in the NH_3-SCR reaction (Xu et al. 2015). The high $Ce^{3+}/(Ce^{3+}+Ce^{4+})$ atomic ratio on Cu-Ce/MZ (39.0%) illustrates the presence of abundant surface oxygen vacancies

Table 1 Textural properties and elemental compositions of catalysts

Samples	S_{BET}[a] (m^2/g)	S_{meso}[b] (m^2/g)	V_{total}[c] (m^3/g)	V_{micro}[b] (m^3/g)	Pore diameter (nm)	Metal loading (wt%)[d]	
						Cu	Ce
MZ	669.4	591.5	0.70	0.03	5.9[e]	–	–
ZSM-5	396.6	–	0.27	–	0.4[f]	–	–
SBA-15	684.7	–	0.78	–	3.9[g]	–	–
Cu-Ce/MZ	512.8	459.0	0.68	0.02	6.2[e]	0.53	2.08
Cu-Ce/ZSM-5	340.3	–	0.26	–	0.4[f]	1.13	0.30
Cu-Ce/SBA-15	404.4	–	0.76	–	5.6[g]	0.68	2.07

[a] Calculated using BET method. [b] Calculated by the t-plot method. [c] Calculated from the adsorption capacity at P/P_0 of 0.99. [d] Determined by ICP-MS. [e] Obtained by applying the DFT method. [f] Obtained by applying the HK method. [g] Obtained by applying the BJH method

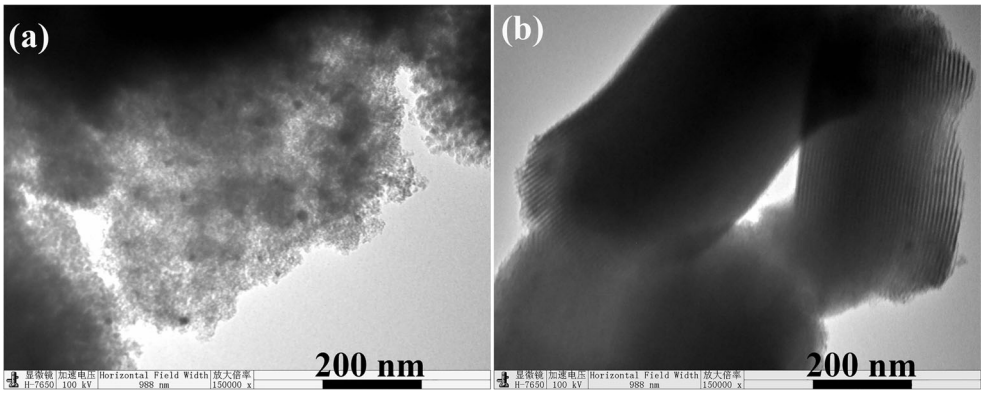

Fig. 3 TEM images of **a** Cu-Ce/MZ and **b** Cu-Ce/SBA-15

and easier activation of reductants in the SCR reaction. Furthermore, the copper or cerium can be highly dispersed in the zeolite framework.

NH_3-TPD results

The surface acidity of catalysts has an important effect on the NH_3-SCR reaction (Brandenberger et al. 2009). The density and intensity of acid sites in Cu-Ce/MZ, Cu-Ce/ZSM-5, and Cu-Ce/SBA-15 are determined by NH_3-TPD (Fig. 5). Two NH_3 desorption peaks are observed in the Cu-Ce/MZ and Cu-Ce/SBA-15 samples. The low-temperature peak at 200 °C is allocated to the weak Brønsted acid sites in the structure. The high-temperature peak at approximately 300 °C is associated with the strong Brønsted acid sites and Lewis acid sites (Si-OH-Al and Cu^{2+}) in the structure (Wang et al. 2014). Furthermore, another desorption peak for Cu-Ce/ZSM-5 at a high temperature (450–600 °C) is related to the new Lewis acid sites created by the Cu species (Worch et al. 2011). Compared with those of the Cu-Ce/ZSM-5 and Cu-Ce/SBA-15 samples, Cu-Ce/MZ shows slightly lower acidity. The strong acidity of Cu-Ce/SBA-15 (Si: Al = 25) originates from the framework aluminum species (Al-OH) due to the introduction of Al (Zhu et al. 2016). Although Cu-Ce/MZ catalyst shows the best NH_3-SCR activity, its acid strength is less than that of the other catalysts. Therefore, it can be concluded that the relationship between acid strength and NH_3-SCR performance is not linear, and the excellent catalytic performance is related to the proper amount of surface acidity (Pang et al. 2014).

NH_3-SCR performance

The catalytic activities of different catalysts for the NH_3-SCR reaction are displayed in Fig. 6. Pure H/MZ exhibits poor

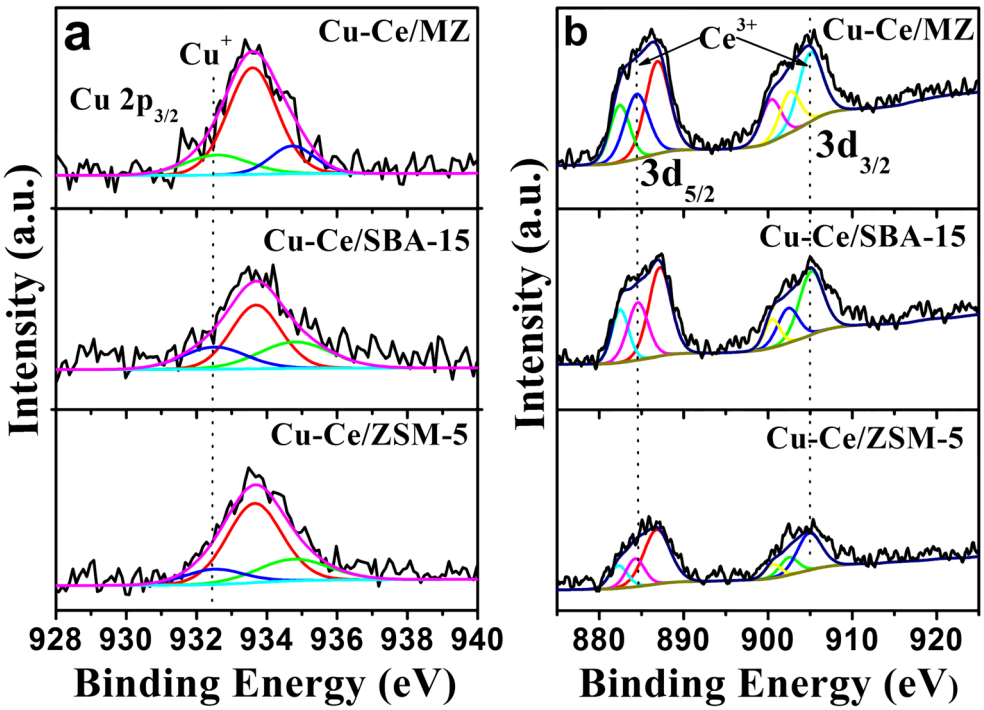

Fig. 4 XPS spectra of the **a** Cu $2p_{3/2}$ and **b** Ce 3d regions for Cu-Ce/MZ, Cu-Ce/SBA-15, and Cu-Ce/ZSM-5

Table 2 The surface compositions of the obtained samples

Samples	Atomic concentration		Atomic ratio	
	Cu (at.%)	Ce (at.%)	$Cu^{+}/(Cu^{+}+Cu^{2+})$ (%)	$Ce^{3+}/(Ce^{3+}+Ce^{4+})$ (%)
Cu-Ce/MZ	0.05	0.11	16.4	39.0
Cu-Ce/SBA-15	0.04	0.09	21.7	40.2
Cu-Ce/ZSM-5	0.06	0.06	13.4	37.3

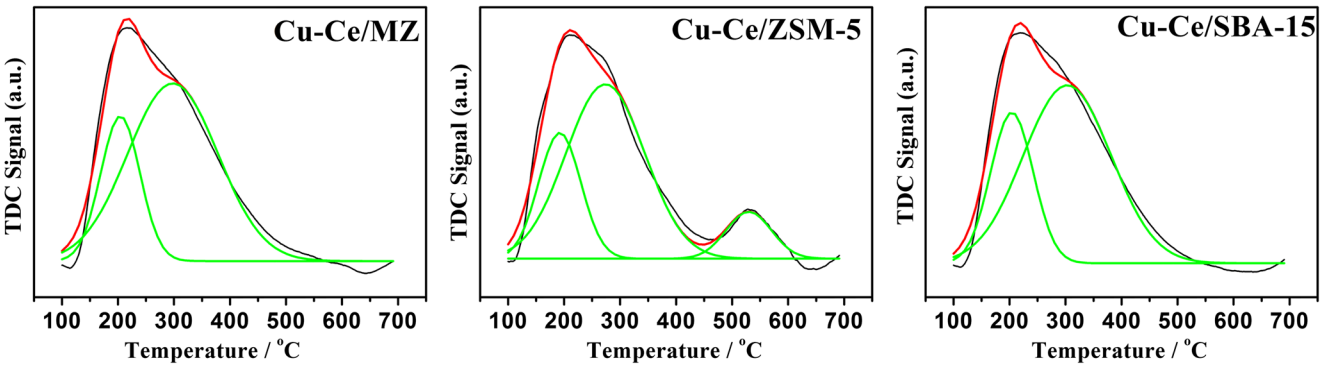

Fig. 5 NH_3-TPD profiles of the Cu-Ce/MZ, Cu-Ce/ZSM-5, and Cu-Ce/SBA-15 samples

activity of about 35% NO_x conversion in the whole temperature range due to lack of redox center, similar to SBA-15 (Zhu et al. 2016) and H-ZSM-5 (Iwasaki et al. 2008). Cu-Ce/MZ displays high NO conversion of 55.9% at 150 °C and 92.7% at 200 °C. For comparison, the catalytic activities of the Cu and Ce loaded on the conventional ZSM-5 and SBA-15 catalysts were also investigated. The Cu-Ce/ZSM-5 exhibits relatively low NO conversion at low temperatures, and maintains NO conversion below 80% until 200 °C. In addition, the activity of Cu-Ce/SBA-15 is also lower than that of Cu-Ce/MZ at low reaction temperatures, with NO conversion of 61.9% at 200 °C. The better catalytic activity of Cu-Ce/MZ can probably be attributed to the presence of mesopores, although the mesopore formation of the catalyst causes the reduction of

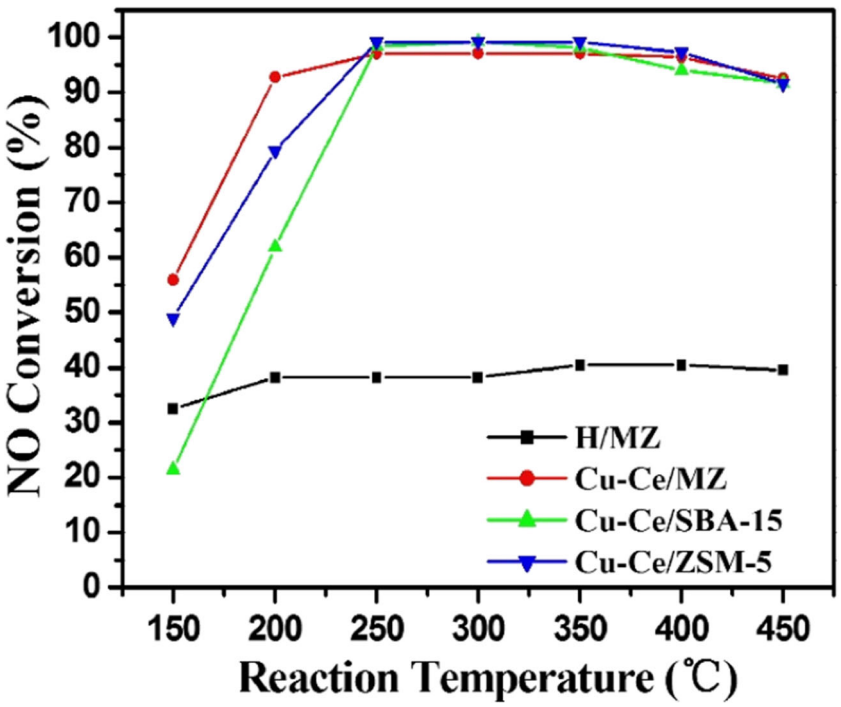

Fig. 6 NO conversion as a function of temperature during standard NH_3-SCR for the Cu-Ce/MZ, Cu-Ce/ZSM-5, and Cu-Ce/SBA-15 samples. The reactant feed contained 500 ppm of NO, 500 ppm of NH_3, 5% O_2, and balanced with N_2 (the total flow rate was 100 mL/min)

crystallinity. The hierarchical micro-mesoporous structure of Cu-Ce/MZ can enhance the diffusion rate of ions, leading to high loading and good dispersion of Cu and Ce species in mesoporous zeolite channels (Yan et al. 2016). Additionally, internal mass transfer limitations are observed in the NH_3-SCR of NO_x over Cu-Ce/ZSM-5, although the molecular sizes of the reactants and products are much smaller than the channel dimension of ZSM-5 (Kustov et al. 2007). Therefore, Cu-Ce/MZ possesses a low kinetic limit and high catalytic activity at low reaction temperatures (< 200 °C) (Gao et al. 2013). Although the SBA-15 support can benefit metal loading and mass transfer due to its mesoporous structure and high surface area, it is not compatible with NH_3-SCR processes due to its poor hydrothermal stability at high temperatures compared with that of the micropore zeolite.

Conclusions

The mesoporous ZSM-5 was used as a support for Cu and Ce species in the NH_3-SCR reaction, and the structure influence and physical-chemical properties of the support on catalytic activity were investigated in this study. Cu-Ce/MZ displayed higher NO conversion at 200 °C than the Cu-Ce/ZSM-5 and Cu-Ce/SBA-15 catalysts. The XRD results and N_2 adsorption-desorption isotherms demonstrated that the high surface area and micro-mesoporous structure of the MZ was successfully maintained when Cu and Ce species were introduced by ion-exchange treatment. ICP-MS and TEM images showed that more active components were dispersed uniformly on the surface of the MZ than those on the microporous ZSM-5 and mesoporous SBA-15. The XPS results and NH_3-TPD profiles illustrated that Cu-Ce/MZ exhibited abundant surface oxygen vacancies and strong acidity. Therefore, the high surface area, more and uniformly distributed active sites, and abundant oxidative species caused the excellent SCR performance of Cu-Ce/MZ.

Funding information This work has been supported by the National Natural Science Foundation of China (51708309), Heilongjiang Province (QC2017065), and the University Nursing Program for Young Scholars with Creative Talents in Heilongjiang Province (UNPYSCT-2018106).

References

Beale AM, Gao F, Lezcano-Gonzalez I, Peden CHF, Szanyi J (2015) Recent advances in automotive catalysis for NO_x emission control by small-pore microporous materials. Chem Soc Rev 44:7371–7405

Boningari T, Pappas DK, Ettireddy PR, Kotrba A, Smirniotis PG (2015) Influence of SiO_2 on M/TiO_2 (M = Cu, Mn, and Ce) formulations for low-temperature selective catalytic reduction of NO_x with NH_3: surface properties and key components in relation to the activity of NO_x reduction. Ind Eng Chem Res 54:2261–2273

Brandenberger S, Kröcher O, Wokaun A, Tissler A, Althoff R (2009) The role of Brønsted acidity in the selective catalytic reduction of NO with ammonia over Fe-ZSM-5. J Catal 268: 297–306

Busca G, Lietti L, Ramis G, Berti F (1998) Chemical and mechanistic aspects of the selective catalytic reduction of NO_x by ammonia over oxide catalysts: a review. Appl Catal B Environ 18:1–36

Chal R, Gérardin C, Bulut M, van Donk S (2011) Overview and industrial assessment of synthesis strategies towards zeolites with mesopores. ChemCatChem 3:67–81

Dusselier M, Davis ME (2018) Small-pore zeolites: synthesis and catalysis. Chem Rev 118:5265–5329

Gao F, Walter E, Washton N, Szanyi J, Peden C (2013) Synthesis and evaluation of Cu-SAPO-34 catalysts for ammonia selective catalytic reduction. 1. Aqueous solution ion exchange. ACS Catal 3:2083–2093

Góra-Marek K, Brylewska K, Tarach KA, Rutkowska M, Jabłońska M, Choi M, Chmielarz L (2015) IR studies of Fe modified ZSM-5 zeolites of diverse mesopore topologies in the terms of their catalytic performance in NH_3-SCR and NH_3-SCO processes. Appl Catal B Environ 179:589–598

Heck RM (1999) Catalytic abatement of nitrogen oxides–stationary applications. Catal Today 53:519–523

Holm MS, Taarning E, Egeblad K, Christensen CH (2011) Catalysis with hierarchical zeolites. Catal Today 168:3–16

Iwamoto M, Furukawa H, Mine Y, Uemura F, S-i M, Kagawa S (1986) Copper(II) ion-exchanged ZSM-5 zeolites as highly active catalysts for direct and continuous decomposition of nitrogen monoxide. J Chem Soc Chem Commun 16:1272–1273

Iwasaki M, Yamazaki K, Banno K, Shinjoh H (2008) Characterization of $Fe/ZSM-5$ $DeNO_x$ catalysts prepared by different methods: relationships between active Fe sites and NH_3-SCR performance. J Catal 260:205–216

Kustov AL, Hansen TW, Kustova M, Christensen CH (2007) Selective catalytic reduction of NO by ammonia using mesoporous Fe-containing HZSM-5 and HZSM-12 zeolite catalysts: an option for automotive applications. Appl Catal B-Environ 76:311–319

Li J, Wang G, Gao C, Lv X, Wang Z, Liu H (2013) Deoxy-liquefaction of laminaria japonica to high-quality liquid oil over metal modified ZSM-5 catalysts. Energy Fuel 27:5207–5214

Liu J, Yu F, Cui L, Zhao Z, Wei Y, Sun Q (2016) Synthesis and kinetics investigation of meso-microporous Cu-SAPO-34 catalysts for the selective catalytic reduction of NO with ammonia. J Environ Sci (China) 48:45–58

Ma J, Weng D, Wu X, Si Z, Wu Z (2013) Highly dispersed iron species created on alkali-treated zeolite for ammonia SCR. Prog in Nat Sci-Mater 23:493–500

Pang L, Fan C, Shao L, Song K, Yi J, Cai X, Wang J, Kang M, Li T (2014) The Ce doping Cu/ZSM-5 as a new superior catalyst to remove NO from diesel engine exhaust. Chem Eng J 253:394–401

Peng C, Liu Z, Horimoto A, Anand C, Yamada H, Ohara K, Sukenaga S, Ando M, Shibata H, Takewaki T, Mukti RR, Okubo T, Wakihara T (2018) Preparation of nanosized SSZ-13 zeolite with enhanced hydrothermal stability by a two-stage synthetic method. Micropor Mesopor Mat 255:192–199

Rutkowska M, Díaz U, Palomares AE, Chmielarz L (2015) Cu and Fe modified derivatives of 2D MWW-type zeolites (MCM-22, ITQ-2 and MCM-36) as new catalysts for $DeNO_x$ process. Appl Catal B Environ 168-169:531–539

Rutkowska M et al (2017) Catalytic performance of commercial Cu-ZSM-5 zeolite modified by desilication in NH_3-SCR and NH_3-SCO processes. Microporous Mesoporous Mater 246:193–206

Serrano DP, Escola JM, Pizarro P (2013) Synthesis strategies in the search for hierarchical zeolites. Chem Soc Rev 42:4004–4035

Shan J-H, Liu X-Q, Sun L-B, Cui R (2008) Cu−Ce bimetal ion-exchanged Y zeolites for selective adsorption of thiophenic sulfur. Energy Fuel 22:3955–3959

Shi A, Wang X, Yu T, Shen M (2011) The effect of zirconia additive on the activity and structure stability of V_2O_5/WO_3-TiO_2 ammonia SCR catalysts. Appl Catal B Environ 106:359–369

Song H, Chang Y, Song H (2015) Deep adsorptive desulfurization over Cu, Ce bimetal ion-exchanged Y-typed molecule sieve. Adsorption 22:139–150

Song L, Chao J, Fang Y, He H, Li J, Qiu W, Zhang G (2016) Promotion of ceria for decomposition of ammonia bisulfate over V_2O_5-MoO_3/TiO_2 catalyst for selective catalytic reduction. Chem Eng J 303: 275–281

Takata T, Tsunoji N, Takamitsu Y, Sadakane M, Sano T (2016) Nanosized CHA zeolites with high thermal and hydrothermal stability derived from the hydrothermal conversion of FAU zeolite. Microporous Mesoporous Mater 225:524–533

Vennestrøm PNR, Grill M, Kustova M, Egeblad K, Lundegaard LF, Joensen F, Christensen CH, Beato P (2011) Hierarchical ZSM-5 prepared by guanidinium base treatment: understanding microstructural characteristics and impact on MTG and NH3-SCR catalytic reactions. Catal Today 168:71–79

Wang D, Zhang L, Li J, Kamasamudram K, Epling WS (2014) NH_3-SCR over Cu/SAPO-34 – zeolite acidity and Cu structure changes as a function of Cu loading. Catal Today 231:64–74

Wang T, Liu H, Zhang X, Guo Y, Zhang Y, Wang Y, Sun B (2017) A plasma-assisted catalytic system for NO removal over CuCe/ZSM-5 catalysts at ambient temperature. Fuel Process Technol 158:199–205

Worch D, Suprun W, Gläser R (2011) Supported transition metal-oxide catalysts for HC-SCR $DeNO_x$ with propene. Catal Today 176:309–313

Wu S, Huang J, Wu T, Song K, Wang H, Xing L, Xu H, Xu L, Guan J, Kan Q (2006) Synthesis, characterization, and catalytic performance of mesoporous Al-SBA-15 for -butylation of phenol. Chin J Catal 27:9–14

Xie Z, Zhou X, Wu H, Chen L, Zhao H, Liu Y, Pan L, Chen H (2016) One-pot hydrothermal synthesis of CuBi co-doped mesoporous zeolite Beta for the removal of NO_x by selective catalytic reduction with ammonia. Sci Rep 6:30132

Xu C, Liu J, Zhao Z, Yu F, Cheng K, Wei Y, Duan A, Jiang G (2015) NH_3-SCR denitration catalyst performance over vanadium–titanium with the addition of Ce and Sb. J Environ Sci 31:74–80

Yan ZF, Li Z, He K, Zhao JS, Lou XR, Zhang JS, Huang W (2016) Hierarchical Fe-ZSM-5 with nano-single-unit-cell for removal of nitrogen oxides. Energ Source Part A 38:315–321

Yue Y, Liu H, Yuan P, Yu C, Bao X (2015) One-pot synthesis of hierarchical FeZSM-5 zeolites from natural aluminosilicates for selective catalytic reduction of NO by NH_3. Sci Rep 5:9270

Zhang R, Liu N, Lei Z, Chen B (2016) Selective transformation of various nitrogen-containing exhaust gases toward N_2 over zeolite catalysts. Chem Rev 116:3658–3721

Zhu L, Qu H, Zhang L, Zhou Q (2016) Direct synthesis, characterization and catalytic performance of Al–Fe-SBA-15 materials in selective catalytic reduction of NO with NH_3. Catal Commun 73:118–122